Fast and Precise 3D Computation of Capacitance of Parallel Narrow Beam MEMS Structures

N. Majumdar, S. Mukhopadhyay

INO Section, Saha Institute of Nuclear Physics, 1/AF, Bidhannagar, Kolkata-700064, India

nayana.majumdar@saha.ac.in, supratik.mukhopadhyay@saha.ac.in

Abstract

Efficient design and performance of electrically actuated MEMS devices necessitate accurate estimation of electrostatic forces on the MEMS structures. This in turn requires thorough study of the capacitance of the structures and finally the charge density distribution on the various surfaces of a device. In this work, nearly exact BEM solutions have been provided in order to estimate these properties of a parallel narrow beam structure found in MEMS devices. The effect of three-dimensionality, which is an important aspect for these structures, and associated fringe fields have been studied in detail. A reasonably large parameter space has been covered in order to follow the variation of capacitance with various geometric factors. The present results have been compared with those obtained using empirical parametrized expressions keeping in view the requirement of the speed of computation. The limitations of the empirical expressions have been pointed out and possible approaches of their improvement have been discussed.

Keywords: MEMS, narrow beam, comb drive, Boundary Element Method (BEM), fringe capacitance.

1. Introduction

The capacitance in MEMS structures has always been an important aspect to be studied from the very beginning of this field of research. Under certain circumstances, the presence of capacitance has turned out to be beneficial while it has been considered as a challenge in some other. In either case, estimation of this capacitance has drawn prime importance reasonably in the design and subsequent use of these devices. The sensitivity, instability and dynamics of a MEMS device depend crucially upon an interplay of electrical and mechanical forces generated within the device. Since the electrostatic force alters the dynamic properties of a MEMS structure and the electrostatic charges redistribute as the structure deforms and thereby change the electrostatic force distribution, a complex electromechanical coupling dictates the performance of the device. This may induce non-linearity in electrostatic force ultimately leading to a pull-in stage. The presence of fringe field may further complicate the situation. Thus an accurate device modeling calls for an efficient electromechanical analysis of the structure which in turn depends crucially on the precision of electrostatic analysis. The electrostatic analysis deals with precise estimation of observables like charge density distribution, total charge content etc. from which the important quantities like capacitance, electrostatic force can be estimated. While the capacitance of a conductor represents its overall charge content and, thus, determines several important properties like electrostatic load distribution on a given structure or induced current, the charge distribution on the conductor finally becomes the most important observable.

The approaches pursued for the electrostatic modeling are predominantly analytical or numerical domain approaches such as the Finite Element Method (FEM) or surface integral approaches such as the Boundary Element Method (BEM) [1]. Among these, the first one, although very fast and accurate, can unfortunately be implemented in a very limited range of two dimensional geometries. There have also been various attempts at providing analytic expression for variation of capacitance for example, in parallel plate structure as a function of the variation of geometrical properties in [2] and the references therein. The numerical approaches on the other hand are capable of taking care of 3D geometry and thus can provide more detailed and realistic estimates. The FEM approach is particularly very flexible in terms of 3D modeling, but demands large computational expenditure for achieving the required accuracy. As a result, the BEM approach has turned out to be the more popular since it produces results of good accuracy with relatively less computational cost. The method has its own drawbacks such as loss of accuracy in the near-field, necessity of special treatment to handle numerical and physical singularities. For example, different special formulations for thick, moderately thin and very thin plate have been devised to compute the necessary properties such as surface charge density and capacitance of a parallel plate structure in order to handle the drawbacks of BEM [3].

Several parametrized formulations have been devised with the help of the numerical methods for fast computation of capacitance in MEMS structures [4], [5], [6] in order to evade the time consuming modeling, computation and other numerical complexities associated with the FEM and BEM. However, these formulations are found to be restricted to specific parameter space as well as 2D geometry.

All the drawbacks associated with FEM and BEM have been removed to a large extent in a novel approach of BEM formulation devised by ourselves using the analytic solution of Green's function form of the potential due to a uniform charge distribution on a boundary element [7], [8]. The solver based on this nearly exact BEM (neBEM) formulations has been found to excel in electrostatic analysis of MEMS yielding very precise results throughout the domain of interest and at

a very close proximity to any surface which are well known handicaps of conventional BEM. In [7], the effect of geometric parameters like thickness of each plate and the gap between them on the charge density distribution and the capacitance of a parallel plate structure were studied. Here, a similar study has been carried out for a narrow beam structure which has already been identified to be strongly influenced by fringe field. For example, very strong fringe field effect has been observed in vertical comb-drive actuator in comparison to parallel plate actuator [9] stressing the need for carrying out such a study. Besides, it has been reported in [10] that even for a plate configuration, when the size of the electrod is not much bigger than the gap, the fringe effect can not be ignored any more. This, of course, was reflected in our earlier studies as well. In addition to studying the effect of the various geometric parameters such as the length, width, height and gap between the two beams on the charge density distribution and capacitance, the accuracy of the various approximate expressions available for fast estimation of capacitance of comb-like structure relevant to MEMS devices has also been checked out. The reasons of failure of such expressions have been discussed and possible ways of improvement have been suggested.

2. **Validation of neBEM**

The results of electrostatic force and capacitance for a parallel plate capacitor provided by neBEM have been compared to that obtained with Coventor's ARCHITECT software and its Parametrized ElectroMechanical model (PEM) [11]. The parallel plate configuration consists of a square plate of side, $L_p = 100\mu m$ and thickness, $t_p = 2\mu m$ separated by a distance H from a square electrode with side, $L_e = 100\mu m$, thickness, $t_e = 0.45\mu m$. The analytical solution of the electrostatic force can be written as follows.

$$F_y = \frac{V^2}{2}\frac{\partial C}{\partial H} = -\frac{V^2}{2}\frac{\epsilon L_p^2}{H^2} \qquad (1)$$

where $\epsilon = \epsilon_0\epsilon_r$; the permittivity constant is $\epsilon_0 = 8.85 \times 10^{-12}F/m$ and $\epsilon_r = 1$ is the relative permittivity of the medium. The ARCHITECT PEM calculation has shown a
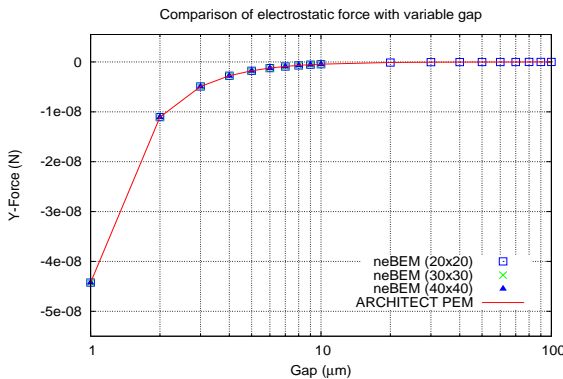

Fig. 1.   Electrostatic force acting on upper plate in a parallel plate configuration

nice agreement with the analytical solution as seen from fig.1. It should be mentioned here that the numerical convergence of the solution while using the BEM needs close inspection. It has been experienced that the higher mesh refinement in BEM which produces convergent capacitance values may not necessarily yield convergent force [12]. In case of neBEM, the numerical convergence of the results has been tested with mesh refinement as well as monitoring the associated charge distributions. It has been found that even with relatively coarse a discretization scheme of 800 elements only, the convergent force values could be achieved which hardly improved by refining the scheme. The results produced with different discretization schemes have been depicted in fig.1. The charge density distribution on the top plate for a gap of $2\mu m$ has been shown in fig.2 as a typical case.
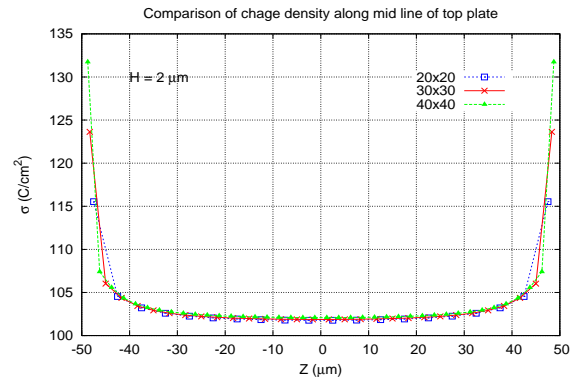

Fig. 2.   Surface charge density distribution on the upper plate of parallel plate configuration with gap $2\mu m$

The capacitance values calculated following the neBEM has shown a difference with what predicted by the PEM calculation as evident from fig.3. It is because the PEM has calculated the capacitance following the analytical expression of parallel plate capacitance as follows

$$C = \frac{\epsilon A}{H} = \frac{\epsilon L_p^2}{H} \qquad (2)$$

which neglect any fringe field contribution while the neBEM has well accounted for that effect in its calculation.

3. **Geometry of Narrow beam structures**

Narrow beam structures of wide geometric variations have been used in MEMS devices. As an example, in fig.4 presented is a comb drive which is actually used as a position sensor in MEMS systems. We have considered a much simplified geometry (Fig.5) which, nevertheless, retains the basic characteristics of such structures. Here, the length, breadth, height of the beam are denoted by l, b and h respectively, and the half-gap between the two beams by g. It can be seen from various references in the published literature that l can range from mm to tens of μm. The breadth, b and height, h can be as small as $2\mu m$ and $4\mu m$. The gap, g also has a wide range of variation from tens of μm to just $1\mu m$. There can be
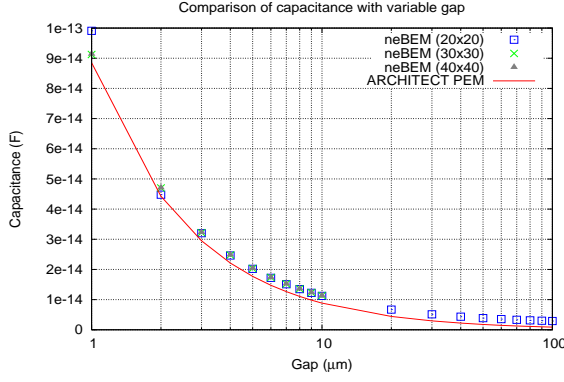
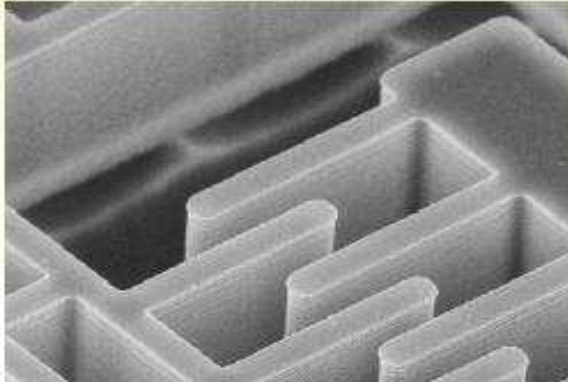Fig. 3. Capacitance calculated for a parallel plate configuration

Fig. 4. Comb drives used as position sensor (Photo courtsey:Kionix Inc.)

devices where these wide variations are even more extended. Instead of trying to cover the whole range of the parameters, we consider narrow beams of $l = 150\mu m$, b varying from $100\mu m$ to $2\mu m$, height $h = 10\mu m$ and g varying from $20\mu m$ to $1\mu m$.

As is obvious from the above range of dimensions, effect of three dimensionality in the narrow beam structures is likely to be even more significant than the parallel plate structures. In many cases of practical interest, even approaches based on reducing the 3D problem to a 2D one, and then recovering the 3D solution as developed in [13] is unlikely to produce good results, especially when, according to some researchers an accuracy of the order of 99% is what should be acceptable in estimating the different parameters related to MEMS devices. Moreover, approaches based on reducing dimensions as above are likely to face problems when the cross-section of the structure varies in the direction of sweep. Thus, these efficient approaches can not be counted on for solving problems of a very general nature. As a result, from the very outset, we prepared ourselves to handle the problem in complete 3D. According to us, rather than evading the 3D nature of the problem, more important is to develop a fast and precise solver. The question of possible parametrization in various ranges, if possible, can of course help in reducing computational
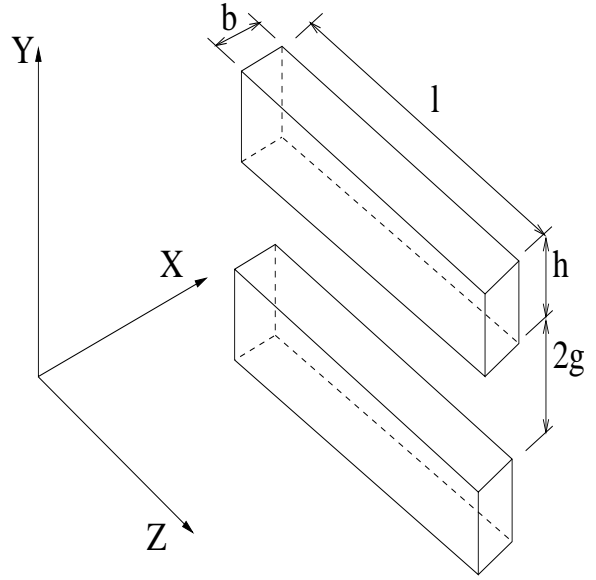

Fig. 5. Narrow beam geometry considered for the present calculations

expenses and also help in saving time to a very great extent. But, even to build proper parametric dependence, we need to solve the 3D problem to an acceptable accuracy.

4. **Results and discussions**

To study the variation of capacitance depending upon various geometric parameters in a parallel narrow beam structure, a convention similar to [4] has been adopted where, in order to facilitate parametrization, the followings have been defined

$$\beta = \frac{h}{b}, \ \ \eta = \frac{h}{g}$$

In addition to the above, another dimensionless parameter has been included.

$$\lambda = \frac{l}{b}$$

According to these parameters, the problem geometry varies from $0.1 \leq \beta \leq 5$, $0.5 \leq \eta \leq 10$ and $1.5 \leq \lambda \leq 75$. The variation can be huge, but a relatively narrow range has been considered to facilitate data interpretation and analysis.

4.1. *Variation of capacitance*

To study the variation of capacitance per unit length with different geometric parameters, the results computed by the neBEM solver has been compared with those calculated using various empirical parametric formulations presented in [4]. In Table 1, the percent deviation incurred by various methods of estimation as well as the neBEM with respect to Method of Moment (MoM) calculation has been tabulated. A column of λ has been added in the table to examine the effect of finite length of the beam which has not been considered in the parametric calculations. It may be recounted that for the present computations, l and h have been kept fixed at $150\mu m$ and $10\mu m$. The parameter b has varied from $100\mu m$ to $2\mu m$,

TABLE 1
COMPARISON OF CAPACITANCE PER UNIT LENGTH DUE TO VARIATION IN GEOMETRIC PARAMETERS

λ	β	η	MoM	Present	[4]	[5]	[6]	Par Plate	Present
1.5	0.1	0.5	8.14	10.43	-1.6	-0.4	-9.2	-38.6	28.13
1.5	0.1	1.0	13.71	16.21	-0.7	¡0.1	-6.5	-27.1	18.23
1.5	0.1	2.5	29.61	32.45	¡0.1	0.7	-4.1	-15.7	9.59
1.5	0.1	5.0	55.38	58.42	0.2	1.0	-3.0	-9.9	5.49
1.5	0.1	10.	106.19	109.34	0.3	1.2	2.2	-6.2	2.91
3.0	0.2	0.5	5.37	6.70	-1.1	-0.4	-17.2	-53.5	24.76
3.0	0.2	1.0	8.42	9.80	-0.4	-0.1	-12.3	-40.7	16.39
3.0	0.2	2.5	16.80	18.29	¡0.1	0.8	-8.0	-25.6	8.89
3.0	0.2	5.0	30.06	31.59	0.3	1.5	-5.6	-16.9	5.09
3.0	0.2	10.	55.86	57.32	0.5	1.9	-4.0	-10.9	2.61
7.5	0.5	0.5	3.61	4.34	¡0.1	-0.8	-34.5	-72.3	20.22
7.5	0.5	1.0	5.12	5.82	0.4	-0.6	-25.7	-61.0	13.67
7.5	0.5	2.5	8.97	9.69	0.4	-0.7	-17.7	-44.3	8.03
7.5	0.5	5.0	14.71	15.41	0.6	2.1	-12.9	-32.1	4.75
7.5	0.5	10.	25.50	26.09	0.9	3.4	-9.1	-21.9	2.31
15.	1.0	0.5	2.96	3.48	0.6	-1.7	-51.9	-83.1	17.57
15.	1.0	1.0	3.96	4.43	0.7	-1.8	-40.3	-74.8	11.87
15.	1.0	2.5	6.29	6.71	0.4	-0.1	-29.3	-60.2	6.68
15.	1.0	5.0	9.52	9.88	0.5	2.2	-22.4	-47.5	3.78
15.	1.0	10.	15.30	14.50	1.1	4.6	-16.4	-34.9	-5.23
30.	2.0	0.5	2.59	2.98	0.8	-2.9	-71.8	-90.4	15.06
30.	2.0	1.0	3.34	3.66	0.7	-3.5	-57.3	-85.0	9.58
30.	2.0	2.5	4.90	5.12	¡0.1	-1.7	-43.8	-74.5	4.49
30.	2.0	5.0	6.88	6.89	¡0.1	1.4	-53.3	-63.7	1.45
30.	2.0	10.	10.16	9.56	0.7	5.4	-27.4	-50.9	-5.90
75.	5.0	0.5	2.34	2.62	0.3	-5.2	Inf	-95.7	11.96
75.	5.0	1.0	2.92	3.14	-0.1	-6.2	-81.5	-93.2	7.01
75.	5.0	2.5	4.03	4.14	-1.4	-4.8	-64.7	-87.6	2.73
75.	5.0	5.0	5.25	5.22	-1.6	-1.0	-55.0	-81.0	0.57
75.	5.0	10.	7.04	6.62	-0.7	4.9	-45.9	-71.6	-5.96

while g from $20\mu m$ to $1\mu m$ (Fig.5. The deviation of the calculations w.r.t MoM values has been plotted as a function of η (inverse gap) in fig.6. The wide variation between the neBEM and parametric results is, in fact, expected because the parametric formulation has been devised for 2D geometry whereas the neBEM takes care of 3D one. Whenever η is small (large gap), for small values of λ (large b for a fixed l), the parametric assumption breaks down resulting in large difference between the 2D and 3D results which reflects the effect of fringing field. However, for the same λ, the difference reduces considerably when the gap between the two structures is reduced (larger η). Obviously, the disagreement between the 2D and 3D results improves when λ becomes larger (smaller b) for a fixed η reflecting the reduction in fringe field effect. The MoM result, and thus those due to [4] are likely to be correct only if the length is much larger than all other dimensions of the beam. This, unfortunately, cannot be very realistic a picture for every narrow beam structure used in MEMS. It is conceivable from the results that all the lengths of the device play important role, and for a true measure of capacitance and related properties, none of these can really be neglected unless we stick to a reasonably narrow parameter window. The window considered above, according to us, is not narrow enough.
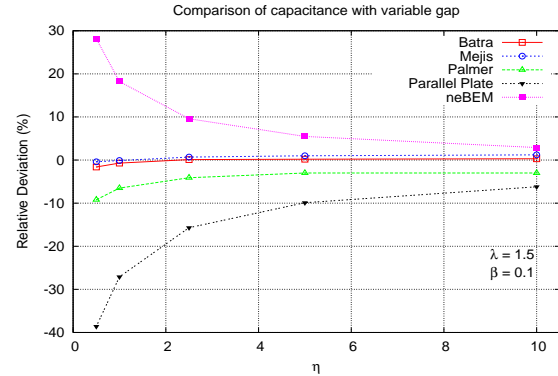

Fig. 6.   Relative deviation calculated capacitance per unit length w.r.t MoM value

4.2. *Variation of charge density distribution*

There is a large increase in charge density near the edges and corners on each surface. Since the electrostatic force depends on this charge density distribution directly, the finite nature of the length can cause error while predicting these important properties of an MEMS device. It may be safer to critically examine the parameter window of interest and only then decide regarding the 2D or 3D nature of the problem. The surface charge density on the surfaces facing the gap and away from it have been illustrated in fig.7 and fig.**??** which shows that the

charge density on surfaces not facing the gap is considerably smaller. In order to emphasize the differences of the charge
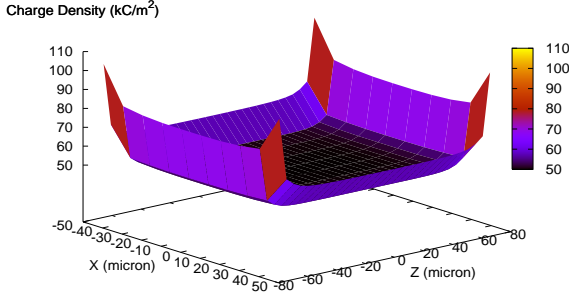

Fig. 7. Surface charge density distribution on a surface facing the gap
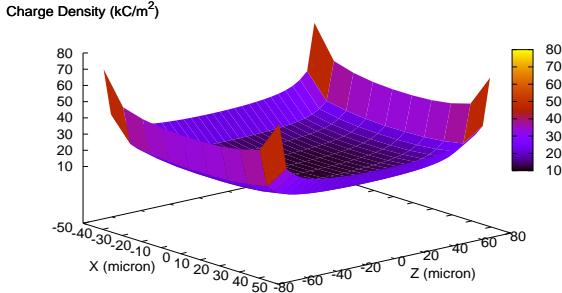

Fig. 8. Surface charge density distribution on a surface away from the gap

Fig. 9. Surface charge density distribution on each surface of the upper beam with gap $20\mu m$

Fig. 10. Surface charge density distribution on each surface of the upper beam with gap $1\mu m$

densities on the various surfaces of the narrow beams, in figs.9 and 10, the charge densities along the mid-sections of each surface of a beam for the largest gap, $g = 20\mu m$ and the smallest gap, $g = 1\mu m$ have been presented. The breadth of the beam has been considered to be $b = 20\mu m$ which is a representative one. Naturally, the charge density is expected to vary as b changes from $100\mu m$ to $2\mu m$. Please note that in these figures, the charge densities on the upper beam of the overall structure have been plotted. According to this figure, the top surface is the one that is away from the gap, while the bottom one faces the gap and the other beam structure. The left and right surfaces are at constant values of X, while the front and back surfaces are at constant values of Z. The variations of charge density for the top and bottom surfaces are along X, left and right surfaces are along Y while for the front and back surfaces are along the X axis. All the distances have been normalized with respect to the length in the corresponding direction for the convenience of both presentation and interpretation.

When the gap is large, the charge density distribution is found to be quite even for many of the surfaces except the surface far away from the gap owing to large fringe field effect.
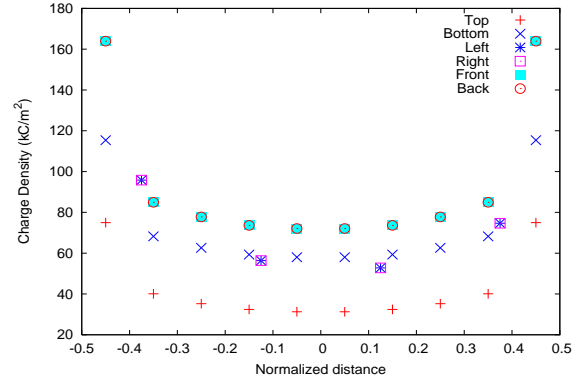
It may be noted here that the symmetric nature of the problem is accurately reflected in the presented results. Thus, the values obtained for left-right and front-back surfaces are completely indistinguishable from each other. The left and right surfaces have an asymmetric distribution of charge density with respect to Y, which also is expected. Lesser values of Y in these cases implies proximity to the gap and thus have larger values of charge density. Moreover, the existence of the edges are clearly visible in all the data points. It should be noticed here that all the surfaces having accumulated quite even charges contribute significantly in the total charge content, thus indicating the consideration of 3D nature of the problem.

The case where the gap between the beams is very small in comparison to all the other dimensions, the average charge density of the surface facing the gap is much larger than the surface charge density of the all the surfaces of the beam implying less fringe field effect. In addition, since the area of this surface is large in comparison to most of the other surfaces, its contribution towards the total charge content of the beam completely dominates over the contribution of the other surfaces. This indicates that at this situation, various electrostatic properties can be approximated by two-dimensional configurations to a large extent.

From the previous discussions, it has seemed to us that the very approach of supplying an expression that will work throughout a large parameter space is bound to face difficulties. It may be far more prudent to divide the parameter space in smaller sub-regions and try to find appropriate relations valid in that sub-space of parameters. In terms of computation, this is not likely to be burdensome as our experience with the neBEM solver suggests. Moreover, the expressions are likely to be far more precise in predicting the capacitance of MEMS structures. However, the very task of finding these expressions may be lengthy and laborious. We plan to carry out a thorough study in this direction in the near future.

5. **Conclusions**

A 3D computation of capacitance of a MEMS parallel narrow beam structure has been presented in this work. The results have been compared with several existing estimates which are essentially 2D in nature. Significant variation in the results have been observed and the reasons behind these discrepancies have been discussed by analyzing the charge densities on the various surfaces of a beam with the variation of the gap in the device. The effect of finite length, even for narrow beams, has been found to be quite large in many areas of the parameter space covered. It has been finally concluded that it may be difficult to find a single expression that will represent the variation of capacitance with geometrical parameters covering a large parameter space.

References

[1] Senturia, S.D., Harris, R.M., Johnson, B.P., Kim, S., Nabors, K., Shulman, M.A. and White, J.K., 1992, "A computer-aided design system for microelectromechanical systems (MEMCAD)", *J Micro Electro Mech Syst*, **1**, pp.3-13.

[2] Leus, V. and Elata, D., 2004, "Fringing field effect in electrostatic actuators", *Technical report ETR-2004-2*, Technion - Israel Institute of Technology, Faculty of Mechanical Engineering, Israel, 15 pages.

[3] Bao, Z. and Mukherjee, S., 2004, "Electrostatic BEM for MEMS with thin conducting plates and shells", *Engg Analysis Bound Elem*, **28**, pp.1427-1435.

[4] Batra,R.C., Porfiri,M. and Spinello,D., 2006, "Electromechanical model of electrically actuated narrow microbeams", *J Microelectromechanical Systems*, Accepted for publication in 2006.

[5] Meijs,N.V.D. and Fokkema,J.T., 1984, "VLSI circuit reconstruction from mask topology", *Integration*, **2**, pp.85-119.

[6] Palmer,H.B., 1937, "Capacitance of a parallel plate capacitor by the Schwartz-Christoffel transformation", *Trans Amer Inst Elect Eng*, **56**, pp.363-366.

[7] Mukhopadhyay, S. and Majumdar, N., 2006, "Computation of 3D MEMS electrostatics using a nearly exact BEM solver", *Engg Analysis Boun Elem*, **30**, pp.687-696.

[8] Mukhopadhyay, S. and Majumdar, N., 2007, "Use of rectangular and triangular elements for nearly exact BEM solutions", *Proc. of Intl. Conf. on Emerging Mechanical Technology- Macro to Nano (EMTM2N-2007)* (ISBN 81-904262-8-1), BITS-PILANI, India, February 16-18, pp.107-114.

[9] Hah, D., Huang, S., Nguyen, H., Chang, H., Tsai, J-C., Wu, M.C. and Toshiyoshi, H., 2006, "Low voltage MEMS analog micromirror arrays with hidden vertical comb-drive actuators", *Solid-State Sensor, Actuator and Microsystems Workshop*, Hilton Head Island, South Carolina, June 2-6, pp.11-14.

[10] Ma, Y., 2004, "Optimal MEMS plate design and control for large channel count optical switches", *Ph.D. Thesis, Faculty of Graduate School of the University of Maryland*, College Park, Maryland, USA .

[11] *http://www.Coventor.com/media/fem_comparisons/parallel_plate.pdf*

[12] Iyer, S., Lakdawala H., Mukherjee T. and Fedder G. K., 2002, "Modeling methodology for a CMOS-MEMS electrostatic comb" *Proceedings of SPIE: Design, Test, Integration and Packaging of MEMS/MOEMS 2002*, **4755**, pp.114-125.

[13] Sirpotdar, A. and Suresh, K., 2006, "A 2D model that accounts for 3D fringing in MEMS devices", *Journal of Engg Analysis Boun Elem*, accepted January 2006.